J. Fluid Mech. (2014), *vol.* 754, *pp.* 161–183.
doi:10.1017/jfm.2014.404

Taylor dispersion and thermal expansion effects on flame propagation in a narrow channel

P. Pearce† and J. Daou

School of Mathematics, University of Manchester, Manchester M13 9PL, UK

(Received 4 February 2014; revised 4 June 2014; accepted 11 July 2014)

We investigate the propagation of a premixed flame subject to thermal expansion through a narrow channel against a Poiseuille flow of large amplitude. This is the first study to consider the effect of a large-amplitude flow, characterised by a Péclet number of order one, $Pe = O(1)$, on a variable-density premixed flame in the asymptotic limit of a narrow channel. It is also the first study on Taylor dispersion in the context of combustion. The relationship between the propagation speed and Péclet number is investigated, with the effect of large flame-front thickness ϵ and activation energy β studied asymptotically in an appropriate distinguished limit. The premixed flame for $\epsilon \to \infty$, with $Pe = O(1)$, is found to be governed by the equation for a planar premixed flame with an effective diffusion coefficient. In this case the premixed flame can be considered to be in the Taylor regime of enhanced dispersion due to a parallel flow. The infinite activation energy limit $\beta \to \infty$ is taken to provide an analytical description of the propagation speed. Corresponding results are obtained for a premixed flame in the constant-density approximation. The asymptotic results are compared to numerical results obtained for selected values of ϵ and β and for moderately large values of the Péclet number. Physical reasons for the differences in propagation speed between constant- and variable-density flames are discussed. Finally, the asymptotic results are shown to agree with those of previous studies performed in the limit $Pe \to 0$.

Key words: combustion, flames, laminar reacting flows

1. Introduction

In this paper we provide the first theoretical study of a variable-density premixed flame propagating through a narrow channel against a Poiseuille flow of large amplitude. Under these conditions, the dependence of the propagation speed of the premixed flame on the Péclet number is investigated. The essential governing parameters are the flame-front thickness ϵ and the amplitude of the flow A (which together define the Péclet number $Pe = A/\epsilon$), as well as the activation energy of the reaction β. The problem studied has relevance to several important areas of research.

The first area concerns premixed flames propagating through narrow channels, which have been the subject of considerable renewed interest in recent years.

† Email address for correspondence: philip.pearce@manchester.ac.uk

In addition to traditional applications such as fire safety in mine shafts (see e.g. Kanury 1975, p. 271), recent applications are concerned with emerging technologies that utilise microscale combustion (see Fernandez-Pello 2002). Related investigations have addressed the development of a suitable analytical methodology, based on a thick-flame asymptotic limit (Daou, Dold & Matalon 2002), the effect of heat loss (Daou *et al.* 2002; Daou & Matalon 2002), the effect of non-unity Lewis numbers (Kurdyumov & Fernandez-Tarrazo 2002; Cui *et al.* 2004; Kurdyumov 2011), the influence of oscillatory flow (Daou & Sparks 2007) and the influence of thermal expansion (Short & Kessler 2009; Kurdyumov & Matalon 2013) under different distinguished limits of the governing parameters. The asymptotic results in the current paper can be considered to be an extension of the results of Daou *et al.* (2002) and Short & Kessler (2009), who studied the same configuration but in the limit of small Péclet number in the constant-density and variable-density cases, respectively. A low value of Pe is not the case, however, in many practical applications (see, for example, the experimental results given in the review article by Bradley (1992) which were obtained for a fixed value of Pe). For this reason the asymptotic analysis in the current study is performed in the limit $\epsilon \to \infty$ with $Pe = O(1)$ and numerical results are obtained for moderately large Péclet numbers.

The second area of research is related, albeit indirectly, to turbulent combustion. At high values of Pe the flame could become turbulent, an aspect of the problem not addressed here. Nevertheless, the results are still useful as a first step towards an understanding of the effects of the small scales in the flow on a turbulent premixed flame; at present there seems to be no analytical description of even laminar premixed flames for arbitrary values of Pe in situations where the flame is thick compared to the length scale of the flow. This latter situation is fundamental to a proper evaluation of Damköhler's second hypothesis (see Damköhler 1940) concerning the effect of small-scale flow on turbulent premixed flames, which has received little attention in the literature. Conversely, there have been many studies on turbulent premixed flames in the flamelet regime of large flow scales compared to the flame thickness (see e.g. Clavin & Williams 1979; Kerstein, Ashurst & Williams 1988; Sivashinsky 1988; Yakhot 1988; Aldredge 1992), which was the subject of Damköhler's first hypothesis. A detailed discussion of the relevance of Damköhler's second hypothesis to turbulent premixed flames can be found in the paper by Daou *et al.* (2002). A thorough review of turbulent combustion in general can be found in the monograph by Peters (2000).

The third area of relevant research is Taylor dispersion, a well-studied topic that began with Taylor's seminal paper discussing the enhanced dispersion of a solute due to a parallel flow in a channel (see Taylor 1953). Taylor investigated a distinguished limit characterised by a small diffusion time in comparison to the advective time; in this limit the depth-averaged concentration of the solute was shown to be governed by a one-dimensional equation with an effective diffusion coefficient D_{eff}, which was found to be larger than the diffusion coefficient D and dependent upon the profile of the parallel flow. Specifically, in the case of a cylindrical channel of radius a and an imposed Poiseuille flow of cross-sectional average $\bar{w}$, Taylor found the effective diffusion coefficient to be given by

$$D_{eff} = D\left(1 + \frac{a^2\bar{w}^2}{48D^2}\right), \tag{1.1}$$

for a solute with diffusion coefficient D.

A comprehensive review of the subject of Taylor dispersion can be found in the book by Brenner & Edwards (1993). Here we simply note that there seem to be

relatively few analytical studies in the literature that investigate Taylor dispersion with a variable-density flow (see Felder *et al.* 2004; Oltean *et al.* 2004; Dentz *et al.* 2006). In these studies the effective diffusion coefficient has been found to be a function of the density. Although there has been a small number of studies on Taylor dispersion in reaction–diffusion equations (e.g. Leconte *et al.* 2008), this paper is the first to discuss Taylor dispersion in the context of combustion. One of the limits taken in the current paper can be considered to characterise the Taylor regime of a premixed flame, whereby the flame is described by the one-dimensional planar premixed flame equation with an effective diffusion coefficient. The determination of the propagation speed (an eigenvalue representing the speed of the travelling premixed flame) is intimately linked to the effective diffusion coefficient in the limit of infinite activation energy. It is surprising that despite this direct link, Taylor dispersion does not yet seem to have been investigated in the context of premixed (laminar or turbulent) combustion.

The main aims of the investigation are: (*a*) to quantify the effect of a small-scale parallel (Poiseuille) flow on the propagation speed of a premixed flame for fixed values of the Péclet number, taking gas expansion into account (see formula (4.14) later); (*b*) to demonstrate that the enhancement of the propagation speed coincides exactly with the Taylor dispersion formula (1.1); (*c*) to provide an analytical confirmation of Damköhler's second hypothesis in our particular case corresponding to a laminar flow with a single scale which is small compared to the flame thickness (see the discussion in the Conclusion). We believe that achieving these aims, albeit in a simplified adiabatic context (such as in Daou & Matalon 2001), as is carried out in this paper, is a contribution of a fundamental nature that will provide a solid basis for future studies accounting for additional realistic effects. These include more complex multi-scale flows and the influence of heat losses, which are not accounted for here to concentrate on the pure interaction between the flow and the flame and to ensure that the analysis is tractable. The practical aspects of heat losses are known to be important in real microcombustion applications; indeed, to minimise the influence of such heat losses, it is well known that thermal management is required experimentally, such as external wall heating (see e.g. Fan *et al.* 2007) or heat recirculation (see e.g. Sitzki *et al.* 2001; Ahn *et al.* 2005); see also the review by Fernandez-Pello (2002).

The paper is structured as follows. In § 2 we formulate the problem. Section 3 consists of an asymptotic analysis in the limit $\epsilon \to \infty$, with $Pe = O(1)$. In § 4 we consider the limit of infinite activation energy, $\beta \to \infty$, in order to provide an analytical description of the propagation speed in terms of Pe. In § 5 we expand and discuss the results of the preceding asymptotic analyses and compare with numerical solutions of the governing equations, with particular emphasis on describing the relationship between the effective propagation speed U_T and Péclet number Pe for several values of the flame-front thickness ϵ and activation energy β. Finally, a summary of the main findings is given in § 6.

2. Formulation

Consider a premixed flame propagating through a channel of height $2L$. Far upstream of the flame a fully developed Poiseuille flow, defined by

$$\tilde{u} = \tilde{A}\left(1 - \frac{\tilde{y}^2}{L^2}\right), \tag{2.1}$$

is prescribed (see figure 1). The governing equations at low Mach number are given by the Navier–Stokes equations coupled to equations for temperature and mass fractions,

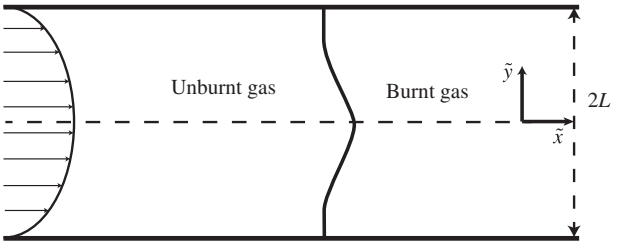

FIGURE 1. An illustration of a premixed flame propagating against a Poiseuille flow in a channel of height $2L$.

along with the ideal gas equation of state. The fluid velocity is given by $(\tilde{u}, \tilde{v})$. The combustion is modelled as a single irreversible one-step reaction of the form

$$F \rightarrow \text{Products} + q, \tag{2.2}$$

where F (assumed to be the deficient reactant) denotes the fuel and q the heat released per unit mass of fuel.

The overall reaction rate $\tilde{\omega}$ is taken to follow an Arrhenius law of the form

$$\tilde{\omega} = \tilde{\rho} B Y_F \exp(-E/R\tilde{T}). \tag{2.3}$$

Here $\tilde{\rho}$, Y_F, R, $\tilde{T}$, B and E are the density, the fuel mass fraction, the universal gas constant, the temperature, the pre-exponential factor and the activation energy of the reaction, respectively. The flame propagates through the channel in the $\tilde{x}$-direction with velocity $-\tilde{U}\boldsymbol{i}$, where U is an eigenvalue to be determined as part of the solution to the problem. With tilda denoting dimensional quantities, scaled non-dimensional variables are introduced using

$$x = \frac{\tilde{x}}{L}, \quad y = \frac{\tilde{y}}{L}, \quad u = \frac{\tilde{u}}{S_L^0}, \quad v = \frac{\tilde{v}}{S_L^0}, \tag{2.4a–d}$$

$$t = \frac{\tilde{t}}{L/S_L^0}, \quad \theta = \frac{\tilde{T} - \tilde{T}_u}{\tilde{T}_{ad} - \tilde{T}_u}, \quad y_F = \frac{Y_F}{Y_{F,u}}, \quad p = \frac{\tilde{p}}{\tilde{\rho}_u \left(S_L^0\right)^2}. \tag{2.5a–d}$$

The unit speed is taken to be

$$S_L^0 = (2Le_F \beta^{-2}(1-\alpha) D_T B \exp(E/R\tilde{T}_{ad}))^{1/2}, \tag{2.6}$$

which is the laminar burning speed of the planar flame for $\beta \gg 1$. Here $\tilde{T}_{ad} \equiv \tilde{T}_u + qY_{Fu}/c_P$ is the adiabatic flame temperature, $\beta \equiv E(\tilde{T}_{ad} - \tilde{T}_u)/R\tilde{T}_{ad}^2$ is the Zeldovich number or non-dimensional activation energy and $\alpha \equiv (\tilde{T}_{ad} - \tilde{T}_u)/\tilde{T}_{ad}$ is the thermal expansion coefficient. The quantities $\tilde{T}_u$, Y_{Fu}, and $\tilde{\rho}_u$ denote the values of the temperature, fuel mass fraction and density in the unburnt gas as $\tilde{x} \rightarrow -\infty$, respectively, while c_P represents the specific heat capacity, which is assumed constant.

In non-dimensional form the governing equations in a coordinate system attached to the flame front, which is travelling in the negative x-direction at speed $U = \tilde{U}/S_L^0$, are given by

$$\frac{\partial \rho}{\partial t} + \boldsymbol{\nabla} \cdot \rho \hat{\boldsymbol{u}} = 0, \tag{2.7}$$

$$\rho\frac{\partial \boldsymbol{u}}{\partial t}+\rho\hat{\boldsymbol{u}}\cdot\boldsymbol{\nabla}\boldsymbol{u}+\boldsymbol{\nabla}p=\epsilon Pr\left(\nabla^2\boldsymbol{u}+\frac{1}{3}\boldsymbol{\nabla}\left(\boldsymbol{\nabla}\cdot\boldsymbol{u}\right)\right), \tag{2.8}$$

$$\rho\frac{\partial\theta}{\partial t}+\rho\hat{\boldsymbol{u}}\cdot\boldsymbol{\nabla}\theta=\epsilon\nabla^2\theta+\frac{\epsilon^{-1}\omega}{1-\alpha}, \tag{2.9}$$

$$\rho\frac{\partial y_F}{\partial t}+\rho\hat{\boldsymbol{u}}\cdot\boldsymbol{\nabla}y_F=\frac{\epsilon}{Le_F}\nabla^2y_F-\frac{\epsilon^{-1}\omega}{1-\alpha}, \tag{2.10}$$

$$\rho=\left(1+\frac{\alpha}{1-\alpha}\theta\right)^{-1}, \tag{2.11}$$

assuming that the thermal diffusivity D_T and the fuel mass diffusion coefficient D_F satisfy $\tilde{\rho}D_T=\tilde{\rho}D_F=$ constant. Here $\hat{\boldsymbol{u}}=\boldsymbol{u}+U\boldsymbol{i}$ and p is the hydrodynamic pressure.

The walls located at $y=-1$ and $y=1$ are considered to be rigid and adiabatic. Symmetry conditions are applied at $y=0$. The boundary conditions are therefore given by

$$\frac{\partial\theta}{\partial y}=\frac{\partial y_F}{\partial y}=\frac{\partial u}{\partial y}=v=\frac{\partial p}{\partial y}=0 \quad \text{at } y=0, \tag{2.12}$$

$$\frac{\partial\theta}{\partial y}=\frac{\partial y_F}{\partial y}=u=v=0 \quad \text{at } y=1, \tag{2.13}$$

$$\theta=0, \quad y_F=1, \quad u=A(1-y^2)=\epsilon Pe(1-y^2), \quad v=0 \quad \text{at } x=-\infty, \tag{2.14a–d}$$

$$\frac{\partial\theta}{\partial x}=\frac{\partial y_F}{\partial x}=\frac{\partial u}{\partial x}=\frac{\partial v}{\partial x}=p=0 \quad \text{at } x=+\infty, \tag{2.15}$$

along with suitable initial conditions. The non-dimensional parameters are defined as

$$\epsilon=\frac{\delta_L}{L}=\frac{D_T/S_L^0}{L}, \quad Pe=\frac{A}{\epsilon}, \tag{2.16a,b}$$

$$Le_F=\frac{D_T}{D_F}, \quad Pr=\frac{\nu}{D_T}, \tag{2.17a,b}$$

which are the non-dimensional flame-front thickness, the Péclet number, the fuel Lewis number and the Prandtl number, respectively. Note that δ_L is the dimensional flame-front thickness given by $\delta_L=D_T/S_L^0$ and A is the non-dimensional amplitude of the imposed Poiseuille flow, $A=\tilde{A}/S_L^0$. Finally, the non-dimensional reaction rate ω is defined as

$$\omega=\frac{\beta^2}{2Le_F}\rho y_F\exp\left(\frac{\beta(\theta-1)}{1+\alpha(\theta-1)}\right). \tag{2.18}$$

The problem is now fully formulated and is given by (2.7)–(2.11), with boundary conditions (2.12)–(2.15). The non-dimensional parameters in this problem are Pe, ϵ, β, α, Pr and Le_F.

Note that by integrating the steady form of (2.9) over the whole domain, using the continuity equation (2.7) with the boundary conditions (2.12)–(2.15) and assuming total fuel consumption downstream, we find

$$U+\bar{u}=\int_0^1\int_{-\infty}^{\infty}\frac{\epsilon^{-1}\omega}{1-\alpha}\mathrm{d}x\mathrm{d}y, \tag{2.19}$$

where $\bar{u}$ is the mean speed of the parallel inflow at $x=-\infty$. Therefore

$$U_T \equiv U + \bar{u} \tag{2.20}$$

appears as an effective propagation speed, as commonly defined in turbulent combustion. In the current study of a Poiseuille flow in a rectangular channel, using the boundary condition (2.14), the effective propagation speed is given by

$$U_T \equiv U + \tfrac{2}{3}\epsilon Pe. \tag{2.21}$$

3. Asymptotic analysis in the limit $\epsilon \to \infty$

To simplify the problem we consider the steady equations with $Le_F = 1$. In this case only the equation for temperature needs to be considered, since $y_F = 1-\theta$. This follows from adding (2.9) and (2.10) and using boundary conditions (2.14).

We now consider the limit $\epsilon \to \infty$ with $Pe = O(1)$, $Pr = O(1)$ and $\beta = O(1)$. The flow amplitude $A = O(\epsilon)$ for $Pe = O(1)$. We introduce a rescaled coordinate

$$\xi = \frac{x}{\epsilon}, \tag{3.1}$$

so that the governing equations (2.7)–(2.11) become

$$\frac{\partial}{\partial \xi}\left(\rho(u+U)\right) + \epsilon \frac{\partial}{\partial y}\left(\rho v\right) = 0, \tag{3.2}$$

$$\rho(u+U)\frac{\partial u}{\partial \xi} + \epsilon\rho v\frac{\partial u}{\partial y} + \frac{\partial p}{\partial \xi} = Pr\left(\frac{4}{3}\frac{\partial^2 u}{\partial \xi^2} + \epsilon^2\frac{\partial^2 u}{\partial y^2} + \frac{\epsilon}{3}\frac{\partial^2 v}{\partial \xi \partial y}\right), \tag{3.3}$$

$$\rho(u+U)\frac{\partial v}{\partial \xi} + \epsilon\rho v\frac{\partial v}{\partial y} + \epsilon\frac{\partial p}{\partial y} = Pr\left(\frac{\partial^2 v}{\partial \xi^2} + \frac{4\epsilon^2}{3}\frac{\partial^2 v}{\partial y^2} + \frac{\epsilon}{3}\frac{\partial^2 u}{\partial \xi \partial y}\right), \tag{3.4}$$

$$\rho(u+U)\frac{\partial \theta}{\partial \xi} + \epsilon\rho v\frac{\partial \theta}{\partial y} = \frac{\partial^2 \theta}{\partial \xi^2} + \epsilon^2\frac{\partial^2 \theta}{\partial y^2} + \frac{\omega}{1-\alpha}, \tag{3.5}$$

$$\rho = \left(1 + \frac{\alpha}{1-\alpha}\theta\right)^{-1}, \tag{3.6}$$

where

$$\omega = \frac{\beta^2}{2}\rho(1-\theta)\exp\left(\frac{\beta(\theta-1)}{1+\alpha(\theta-1)}\right). \tag{3.7}$$

These equations are subject to the boundary conditions (2.12) and (2.13), with

$$\theta = 0, \quad u = A(1-y^2) = \epsilon Pe(1-y^2), \quad v = 0 \quad \text{at } \xi = -\infty, \tag{3.8a–c}$$

$$\frac{\partial \theta}{\partial \xi} = \frac{\partial u}{\partial \xi} = \frac{\partial v}{\partial \xi} = p = 0 \quad \text{at } \xi = +\infty. \tag{3.9}$$

We now introduce expansions for $\epsilon \to \infty$ in the form

$$\left.\begin{aligned} &U = -\tfrac{2}{3}\epsilon Pe + U_0 + \epsilon^{-1}U_1 + \cdots, \\ &u = \epsilon u_0 + u_1 + \cdots, \quad v = v_0 + \epsilon^{-1}v_1 + \cdots, \\ &\theta = \theta_0 + \epsilon^{-1}\theta_1 + \cdots, \quad p = \epsilon^3 p_0 + \epsilon^2 p_1 + \cdots. \end{aligned}\right\} \tag{3.10}$$

Note that here U_0 is the leading-order approximation to the effective flame speed U_T, defined in (2.20). Note also that the horizontal velocity component u is $O(\epsilon)$, due to the imposed Poiseuille flow at $\xi = -\infty$ given by (3.8), while the vertical component of the velocity v is taken to be $O(1)$ to balance the two terms in the continuity equation (3.2).

Substituting (3.10) into (3.2)–(3.5), we obtain to leading order

$$\frac{\partial}{\partial \xi}\left(\rho_0\left(u_0 - \frac{2}{3}Pe\right)\right) + \frac{\partial}{\partial y}\left(\rho_0 v_0\right) = 0, \tag{3.11}$$

$$\frac{\partial p_0}{\partial \xi} = Pr\frac{\partial^2 u_0}{\partial y^2}, \tag{3.12}$$

$$\frac{\partial p_0}{\partial y} = 0, \tag{3.13}$$

$$\frac{\partial^2 \theta_0}{\partial y^2} = 0. \tag{3.14}$$

Equations (3.13) and (3.14) can be integrated with respect to y to give $p_0 = p_0(\xi)$ and $\theta_0 = \theta_0(\xi)$, after using the boundary condition (2.12) on θ_0, so that $\rho_0 = \rho_0(\xi)$ from (3.6).

Now, using a similar method to Short & Kessler (2009), we look for a separable solution for $u_0(\xi, y)$ in the form

$$u_0(\xi, y) = \hat{u}_0(y)\check{u}_0(\xi). \tag{3.15}$$

Substitution of (3.15) into (3.12) gives

$$\frac{\partial^2 \hat{u}_0}{\partial y^2} = \frac{1}{\check{u}_0 Pr}\frac{\partial p_0}{\partial \xi} = -2C, \tag{3.16}$$

where C is a constant. Equation (3.16) can be integrated twice with respect to y, using the boundary conditions (2.12) and (2.13), to yield

$$\hat{u}_0(y) = C(1 - y^2), \tag{3.17}$$

so that

$$u_0(\xi, y) = \check{u}_0(\xi)(1 - y^2), \tag{3.18}$$

where C has been absorbed into $\check{u}_0(\xi)$.

Integrating equation (3.11) with respect to y from $y = 0$ to $y = 1$, we obtain

$$\frac{\partial}{\partial \xi}\left(\rho_0(\xi)\left(\frac{2}{3}\check{u}_0(\xi) - \frac{2}{3}Pe\right)\right) = 0, \tag{3.19}$$

after using boundary conditions (2.12) and (2.13) on v_0. Equation (3.19) implies that

$$\tfrac{2}{3}\rho_0(\xi)(\check{u}_0(\xi) - Pe) = \tfrac{2}{3}(\check{u}_0(\xi \to -\infty) - Pe) = 0, \tag{3.20}$$

using the fact that $\rho_0(\xi \to -\infty) = 1$ from (3.6) and boundary condition (3.8). Thus $\check{u}_0(\xi) = Pe$, so that

$$u_0 = Pe(1 - y^2). \tag{3.21}$$

Equation (3.11) can then integrated with respect to y, using (3.21) and condition (2.12), to yield

$$v_0 = -\frac{1}{\rho_0}\frac{\partial \rho_0}{\partial \xi}\frac{Pe}{3}(y - y^3). \tag{3.22}$$

Now, at $O(\epsilon)$ in (3.5) we have

$$\rho_0 \left(u_0 - \frac{2}{3}Pe\right)\frac{\partial \theta_0}{\partial \xi} = \frac{\partial^2 \theta_1}{\partial y^2}, \tag{3.23}$$

which, after using (3.21) and condition (2.12), can be integrated twice with respect to y to give

$$\theta_1 = \rho_0 \frac{\partial \theta_0}{\partial \xi} Pe \left(\frac{y^2}{6} - \frac{y^4}{12}\right) + \breve{\theta}_1(\xi). \tag{3.24}$$

Next we look to $O(1)$ in (3.2) to find

$$\frac{\partial}{\partial \xi}\left(\rho_1 \left(u_0 - \frac{2}{3}Pe\right)\right) + \frac{\partial}{\partial \xi}\left(\rho_0 \left(u_1 + U_0\right)\right) + \frac{\partial}{\partial y}\left(\rho_0 v_1\right) + \frac{\partial}{\partial y}\left(\rho_1 v_0\right) = 0. \tag{3.25}$$

Equation (3.25) can be integrated first with respect to y from $y = 0$ to $y = 1$, utilising the boundary conditions (2.12) and (2.13) on v_0, and then with respect to ξ to give

$$\int_0^1 \left(\rho_1 \left(u_0 - \frac{2}{3}Pe\right)\right) \mathrm{d}y + \int_0^1 \left(\rho_0 \left(u_1 + U_0\right)\right) \mathrm{d}y = K. \tag{3.26}$$

To evaluate K, we use boundary conditions (3.8) to obtain

$$\begin{aligned} K \;=\; & \int_0^1 \left(\rho_1(\xi \to -\infty)\left(u_0(\xi \to -\infty) - \frac{2}{3}Pe\right)\right) \mathrm{d}y \\ & + \int_0^1 \left(\rho_0(\xi \to -\infty)\left(u_1(\xi \to -\infty) + U_0\right)\right) \mathrm{d}y = U_0. \end{aligned} \tag{3.27}$$

Finally, at $O(1)$ of (3.5) we have

$$\begin{aligned} & \rho_0 \left(u_1 + U_0\right)\frac{\partial \theta_0}{\partial \xi} + \rho_1 \left(u_0 - \frac{2}{3}Pe\right)\frac{\partial \theta_0}{\partial \xi} + \rho_0 \left(u_0 - \frac{2}{3}Pe\right)\frac{\partial \theta_1}{\partial \xi} + \rho_0 v_0 \frac{\partial \theta_1}{\partial y} \\ & = \frac{\partial^2 \theta_0}{\partial \xi^2} + \frac{\partial^2 \theta_2}{\partial y^2} + \frac{\omega_0}{1 - \alpha}, \end{aligned} \tag{3.28}$$

where $\omega_0(\xi) = \omega(\theta_0, \rho_0)$. Integrating (3.28) with respect to y from $y = 0$ to $y = 1$, taking into account the boundary conditions (2.12) and (2.13) on θ and substituting (3.21), (3.22), (3.24), (3.26) and (3.27), we obtain

$$U_0 \frac{\partial \theta_0}{\partial \xi} - \frac{\partial}{\partial \xi}\left(\left(1 + \frac{8}{945}Pe^2 \rho_0^2\right)\frac{\partial \theta_0}{\partial \xi}\right) = \frac{\omega_0}{1 - \alpha}, \tag{3.29}$$

with

$$\left.\begin{aligned} \rho_0 &= \left(1 + \frac{\alpha}{1 - \alpha}\theta_0\right)^{-1}, \\ \omega_0 &= \frac{\beta^2}{2}\rho_0 \left(1 - \theta_0\right) \exp\left(\frac{\beta \left(\theta_0 - 1\right)}{1 + \alpha \left(\theta_0 - 1\right)}\right), \end{aligned}\right\} \tag{3.30}$$

subject to the boundary conditions

$$\theta_0(-\infty) = 0, \quad \theta_{0\xi}(+\infty) = 0. \tag{3.31a,b}$$

This shows that in the limit $\epsilon \to \infty$, with $Pe = O(1)$, the problem of a variable-density premixed flame in a two-dimensional channel can be reduced to a one-dimensional boundary value problem. Equation (3.29) is the equation that would describe a premixed flame propagating through a one-dimensional channel with an effective diffusion coefficient

$$D_{eff} = D_T \left(1 + \frac{8}{945} Pe^2 \frac{\tilde{\rho}^2}{\tilde{\rho}_u^2}\right). \tag{3.32}$$

This is an important result because it corresponds to a generalised form (accounting for variable density effects) of the effective diffusion coefficient found when studying the effect of a Poiseuille flow on mixing in the non-reactive Taylor dispersion problem, originally investigated by Taylor (1953). A premixed flame in the limit $\epsilon \to \infty$, with $Pe = O(1)$ can be therefore considered to be in the Taylor dispersion regime.

The boundary value problem (3.29)–(3.31) will be solved numerically in § 5 to provide a description of the relationship between U_T and Pe. These results will also be compared to those of numerical solutions of the full problem. Firstly, however, we will proceed to study the limit $\beta \to \infty$ in order to find an analytical solution for U_T.

4. Explicit solution for large activation energy $\beta \to \infty$

Here we consider the solution to the problem (3.29)–(3.31) in the limit of infinite activation energy $\beta \to \infty$. Following a well-known approach in this limit, the reaction is confined to a thin layer of thickness $O(\beta^{-1})$. The domain can therefore be split into two outer zones (which we refer to as the preheat zone and the burnt gas) and an inner zone (the reaction zone). We use the condition $\theta_0(\xi \to \infty) = 1$, which follows from the total completion of the reaction far downstream.

In the outer zones the reaction rate is set to zero so that, from (3.29),

$$U_0 \frac{\mathrm{d}\theta_0}{\mathrm{d}\xi} - \frac{\mathrm{d}}{\mathrm{d}\xi}\left(\left(1 + \frac{8}{945} Pe^2 \rho_0^2\right) \frac{\mathrm{d}\theta_0}{\mathrm{d}\xi}\right) = 0, \tag{4.1}$$

where $\rho_0 = \rho(\theta_0)$. The solution to this equation in the burnt gas is found to be

$$\theta_0 = 1, \tag{4.2}$$

while in the preheat zone we have, denoting $P = 8Pe^2/945$ and $\tilde{\alpha} = \alpha/(1-\alpha)$,

$$\frac{(U_0\theta_0)^{(P+1)/U_0}}{(1+\tilde{\alpha}\theta_0)^{P/U_0}} \exp\left(\frac{P}{U_0\,(1+\tilde{\alpha}\theta_0)}\right) = C_1 \exp(\xi), \tag{4.3}$$

on using the condition (3.8). The constant C_1 can be determined by choosing the origin where the outer profiles intersect, since the problem is translationally invariant in the ξ-direction. This gives

$$C_1 = (1+\tilde{\alpha})^{-P/U_0} \exp\left(\frac{P}{(1+\tilde{\alpha})U_0}\right) U_0^{(1+P)/U_0}. \tag{4.4}$$

The propagation speed U_0 can now be determined by matching with the inner solution. Since the reaction layer is of thickness $O(\beta^{-1})$, in the inner region we let

$$X = \frac{\xi}{\beta^{-1}}, \quad \theta_0^{inner} = \Theta(X) = 1 + \beta^{-1}\Theta^1 + O(\beta^{-2}). \tag{4.5a,b}$$

Then to leading order we have

$$\Theta^1_{XX} - \Lambda\Theta^1 \exp(\Theta^1) = 0, \tag{4.6}$$

where

$$\Lambda = \left(2\,(1+\tilde{\alpha})\left(1+\frac{P}{(1+\tilde{\alpha})^2}\right)\sqrt{1-\alpha}\right)^{-1}. \tag{4.7}$$

The boundary conditions to (4.6) are found by matching with the outer solutions using the formula

$$\theta_0^{inner}\,(X\to\pm\infty) = \theta_0^{outer}(\xi\to 0^{\pm}). \tag{4.8}$$

Matching with the solution in the burnt gas, given by (4.2), yields

$$\Theta^1\,(X\to+\infty) = 0. \tag{4.9}$$

Now, noting from (4.5) and (4.8) that

$$\theta_0(\xi\to 0^-) = 1+\beta^{-1}\Theta^1\,(X\to-\infty) + O(\beta^{-2}), \tag{4.10}$$

we expand (4.3) for the temperature in the unburnt gas as $\xi\to 0$ to find

$$\Theta^1\,(X\to-\infty) = \frac{(1+\tilde{\alpha})^2\,U_0}{(1+\tilde{\alpha})^2+P}X. \tag{4.11}$$

Now U_0 can be found by integrating (4.6) subject to the boundary conditions (4.9) and (4.11). Multiplying (4.6) by Θ^1_X and integrating with respect to X from $X=-\infty$ to $X=+\infty$ yields

$$\left[\frac{\left(\Theta^1_X\right)^2}{2}\right]_{X=-\infty}^{X=+\infty} = \int_{\Theta^1(-\infty)}^{\Theta^1(+\infty)} \Lambda\Theta^1\exp\left(\Theta^1\right)\mathrm{d}\Theta^1. \tag{4.12}$$

Thus, using (4.9) and (4.11),

$$\left(\frac{(1+\tilde{\alpha})^2\,U_0}{(1+\tilde{\alpha})^2+P}\right)^2 = 2\Lambda, \tag{4.13}$$

so that

$$U_0 = \sqrt{1+\frac{8}{945}Pe^2\,(1-\alpha)^2}. \tag{4.14}$$

This equation gives the leading-order approximation U_0 to the effective flame speed U_T for a given value of Pe in the limit $\epsilon\to\infty$, $\beta\to\infty$, with $Pe = O(1)$.

4.1. *Constant-density results*

The asymptotic results found for a variable-density premixed flame can be similarly derived in the simpler case of a constant-density premixed flame. The boundary value problem corresponding to (3.29)–(3.31), corresponding to $\epsilon\to\infty$ with $Pe = O(1)$, is

$$U_0\frac{\partial\theta_0}{\partial\xi} - \left(1+\frac{8}{945}Pe^2\right)\frac{\partial^2\theta_0}{\partial\xi^2} = \omega_0, \tag{4.15}$$

with

$$\omega_0 = \frac{\beta^2}{2}\,(1-\theta_0)\exp\left(\frac{\beta\,(\theta_0-1)}{1+\alpha\,(\theta_0-1)}\right), \tag{4.16}$$

subject to the boundary conditions

$$\theta_0(-\infty) = 0, \quad \theta_{0\xi}(+\infty) = 0. \tag{4.17a,b}$$

In the limit $\beta \to \infty$, this problem has the solution

$$U_0 = \sqrt{1 + \frac{8}{945} Pe^2}. \tag{4.18}$$

4.2. *Cylindrical channel results*

A similar asymptotic analysis to the one above can be performed (see the appendix A) for a premixed flame propagating through a cylindrical channel of diameter $2L$ with an imposed Poiseuille flow. As in the case of a rectangular channel it is found that the flame is governed by the equation for a planar premixed flame with an effective diffusion coefficient, in this case given by

$$D_{eff} = D_T \left(1 + \frac{1}{192} Pe^2 \frac{\tilde{\rho}^2}{\tilde{\rho}_u^2}\right) \tag{4.19}$$

in the variable-density case, and

$$D_{eff} = D_T \left(1 + \frac{1}{192} Pe^2\right) \tag{4.20}$$

in the constant-density case. Using the definition of the Péclet number the constant-density result can be written in dimensional form as

$$D_{eff} = D_T \left(1 + \frac{L^2 \bar{u}^2}{48 D_T^2}\right), \tag{4.21}$$

where $\bar{u} = \tilde{A}/2$ is the cross-sectional average of the imposed Poiseuille flow. The result (4.21) is exactly the result (1.1) found by Taylor (1953) in his original paper.

5. Further results and discussion

In this section we compare the results of the asymptotic analyses undertaken in previous sections with the results of numerical computations. The main aim is to examine the relationship between the effective propagation speed U_T, defined in (2.20), and the Péclet number Pe for several values of the flame-front thickness ϵ and activation energy β, in both the variable-density and constant-density cases.

5.1. *Numerical procedure*

The numerical results are obtained by solving the steady form of (2.7)–(2.11) with boundary conditions (2.12)–(2.15) using the software package Comsol Multiphysics. This software has been extensively tested in combustion applications including our previous publications (see Pearce & Daou 2013*a*,*b*). The problem is entered into the partial differential equation (PDE) interface in Comsol, which uses a finite element discretisation to transform the set of nonlinear PDEs into a set of nonlinear algebraic equations in which the propagation speed U_T appears as an additional unknown (eigenvalue). These equations, augmented by the requirement that the temperature is prescribed at the origin (an additional equation needed to determine the eigenvalue U_T), are then solved using an affine invariant form of the damped Newton method, as described by Deuflhard (1974). In the constant-density case we solve (2.9) with $u = \epsilon Pe(1 - y^2)$, $v = 0$, $\rho = 1$ and the reaction term replaced by $\epsilon^{-1}\omega$. The domain is covered by a non-uniform grid of approximately 200 000 triangular elements, with

local refinement around the reaction zone. Various tests are performed to ensure the results are independent of the mesh. A channel of length $x = 30\epsilon$ is taken to approximate an infinitely long channel. Throughout this section we let $Le_F = 1$, $Pr = 1$ and $\alpha = 0.85$ unless otherwise stated. The numerical calculations are performed for a fixed value of the activation energy, $\beta = 10$. For each Pe the value of U_T is scaled by the value of U calculated numerically for $Pe = 0$. Finally the boundary value problems (3.29)–(3.31) and (4.15)–(4.17), derived in the limit $\epsilon \to \infty$, are solved using the BVP4C solver in Matlab, which uses a Lobatto IIIa method (see Shampine, Kierzenka & Reichelt 2000).

5.2. *Comparison of the asymptotic and numerical results*

Figures 2(*a*) and 2(*b*) summarise both the asymptotic and numerical results in the constant-density case and variable-density case, respectively. Plotted are: (i) the solutions to the boundary value problems (3.29)–(3.31) and (4.15)–(4.17), derived in the limit $\epsilon \to \infty$, $Pe = O(1)$, for several values of β; (ii) the asymptotic results (4.14) and (4.18), derived in the limit $\epsilon \to \infty$, $\beta \to \infty$, $Pe = O(1)$; (iii) the results of numerical solutions of the full problem, given by (2.7)–(2.11) and boundary conditions (2.12)–(2.15), for large values of both ϵ and β.

It can be seen that in both the constant- and variable-density cases there is strong agreement between the numerical results calculated for high values of ϵ with $\beta = 10$ and the asymptotic results derived in the limit $\epsilon \to \infty$ for $\beta = 10$. It can also be seen that in both cases the asymptotic results derived in the limit $\epsilon \to \infty$ (for a chosen value of β) approach the results derived in the limit $\epsilon \to \infty$, $\beta \to \infty$ when β is increased, as expected. Comparing the figures shows that a finite value of the activation energy β has a larger effect on the propagation speed in the variable-density case than in the constant-density case.

A further comparison of figures 2(*a*) and 2(*b*) shows that Pe has a significantly larger effect on the propagation speed in the constant-density case than when thermal expansion is taken into account. This can be explained by considering the perturbation to the flame shape using the method of Daou & Matalon (2002) and Short & Kessler (2009). Using the fact that $\theta_0 = \theta_0(\xi)$ and (3.24) we have

$$\theta = \theta_0(\xi) + \epsilon^{-1}\left(\rho_0 \frac{\partial \theta_0}{\partial \xi} Pe\left(\frac{y^2}{6} - \frac{y^4}{12}\right) + \breve{\theta}_1(\xi)\right) + O(\epsilon^{-2}). \tag{5.1}$$

Now, let ξ^* be the location at which the leading-order temperature takes the constant value θ_0^*. Defining the perturbation $\xi = \xi^* + \epsilon^{-1}\xi'$, and letting * denote the value of a variable at ξ^*, so that

$$\theta(\xi^* + \epsilon^{-1}\xi') = \theta_0^* + \epsilon^{-1}\left(\theta_1^*(y) + \xi' \frac{\partial \theta_0^*}{\partial \xi}\right) + O(\epsilon^{-2}), \tag{5.2}$$

we obtain the value of ξ' for which $\theta(\xi^* + \epsilon^{-1}\xi') = \theta_0^*$ as

$$\xi' = -\rho_0^* Pe\left(\frac{y^2}{6} - \frac{y^4}{12}\right) - \frac{\breve{\theta}_1^*}{\theta_{0\xi}^*}. \tag{5.3}$$

Finally, the relative distance between the temperature reaching θ_0^* at $y = 0$ and reaching the same value at $y = 1$ is given by

$$\xi_r' = \frac{\rho_0^* Pe}{12}, \tag{5.4}$$

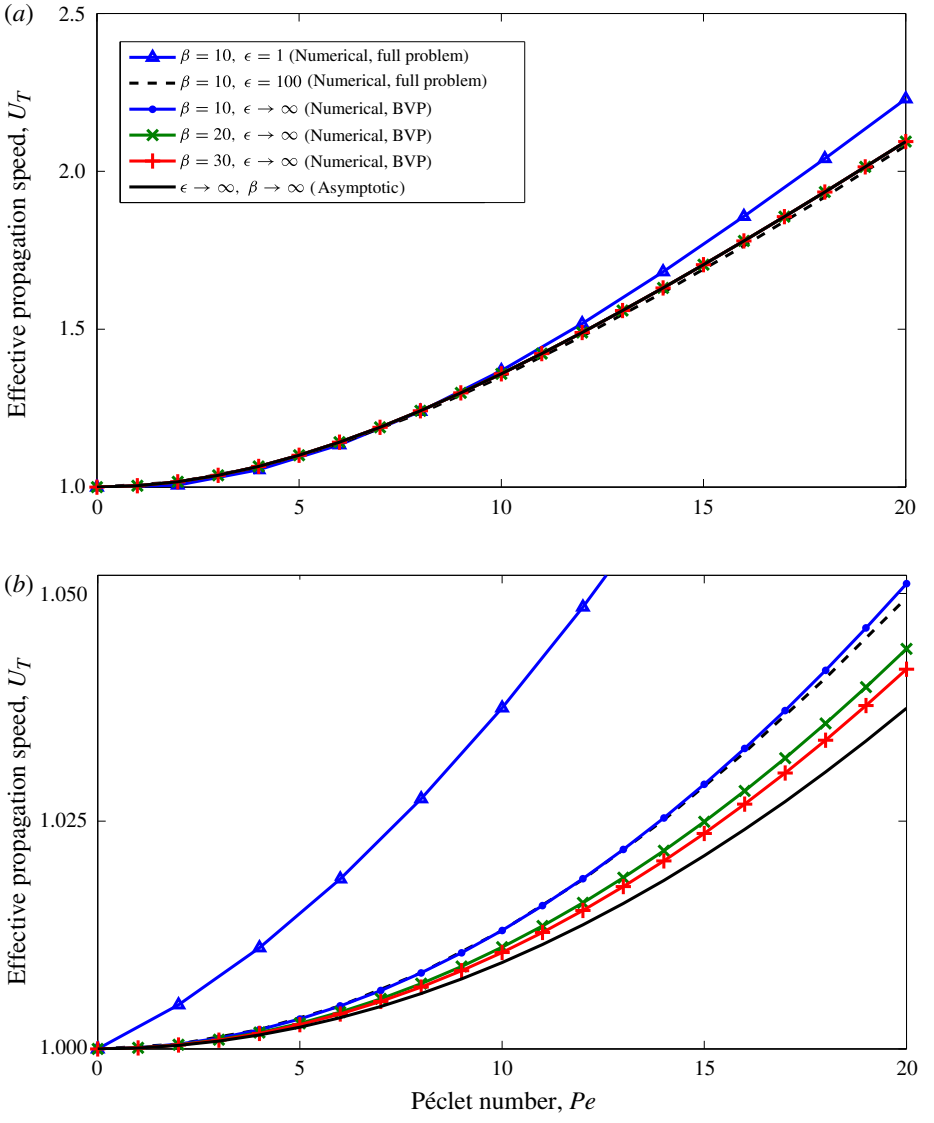

FIGURE 2. (Colour online) Summary of asymptotic and numerical results in (*a*) constant-density case and (*b*) variable-density case. Numerical simulations of the full system (2.7)–(2.15) are performed for $\alpha = 0.85$, $\beta = 10$ and $Pr = 1$. Numerical solutions of the boundary value problem (BVP) (3.29)–(3.31) are calculated for $\alpha = 0.85$ and selected values of β.

which gives a measure of the deformation to the flame due to the flow. The equivalent of (5.4) in the constant-density case is given by

$$\xi'_{r,const} = \frac{Pe}{12}. \tag{5.5}$$

Thus since $\rho_0 < 1$, we have $\xi'_r < \xi'_{r,const}$ from (5.4) and (5.5) and therefore the deformation to the flame shape is smaller in the variable-density case. This means that the effective propagation speed U_T, which gives a measure of the burning rate of

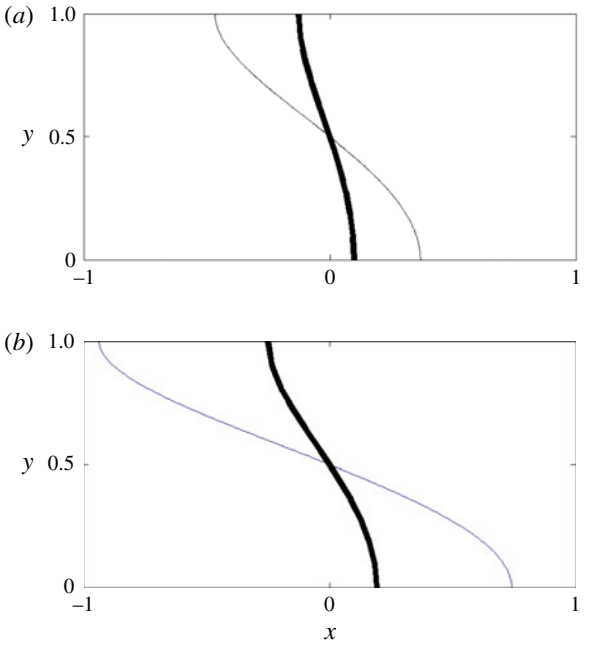

FIGURE 3. Flame shape (represented by the line $\theta = 0.5$) for $\epsilon = 10$, $\beta = 10$ and (*a*) $Pe = 10$, (*b*) $Pe = 20$ in the constant-density (thin line) and variable-density (thick line) cases.

the flame, is expected to be less in the variable-density case. Note that in the $Pe \to 0$ analysis of Short & Kessler (2009), the flame deformation was found to be larger in the variable-density case than the constant-density case for values of Pe giving a propagation speed $U > 0$, and smaller in the variable-density case when $U < 0$. Since $U = U_T - (2/3)\epsilon Pe$, where $U_T = O(1)$ and $\epsilon \to \infty$, the propagation speed U is always expected to be negative in our study and so the results (5.4) and (5.5) agree with those of Short & Kessler (2009).

An illustration of the numerically calculated flame shape for selected values of the Péclet number in both the constant-density and variable-density cases is given in figure 3, which shows that the deformation to the flame shape is indeed larger in the variable-density case, as found in (5.4) and (5.5).

The flame behaviour and its interaction with the flow is further illustrated in figures 4 and 5, corresponding to numerical simulations. Figure 4(*a*) shows a contour plot of the temperature θ; also shown is the velocity field induced by thermal expansion, namely $(u - \epsilon Pe(1 - y^2), v)$. This is plotted rather than the full velocity field (u, v) for clarity since the imposed Poiseuille flow is large compared to the induced flow, which is consistent with the asymptotic findings (see (3.21)). Figures 4(*b*) and 4(*c*) provide contour plots of the horizontal and vertical components of the induced flow, respectively. It is seen that for a fixed value of x, the maximum of the horizontal component of the induced flow is located at the centreline $y = 0$, and the maximum of the vertical component is located around $y = 0.5$. Figures 5(*c*) and 5(*d*) plot these horizontal and vertical components at $y = 0$ and $y = 0.5$, respectively for selected values of Pe. Corresponding plots of the temperature θ and the reaction rate ω along the centreline $y = 0$ are shown in figures 5(*a*) and 5(*b*). Figure 5

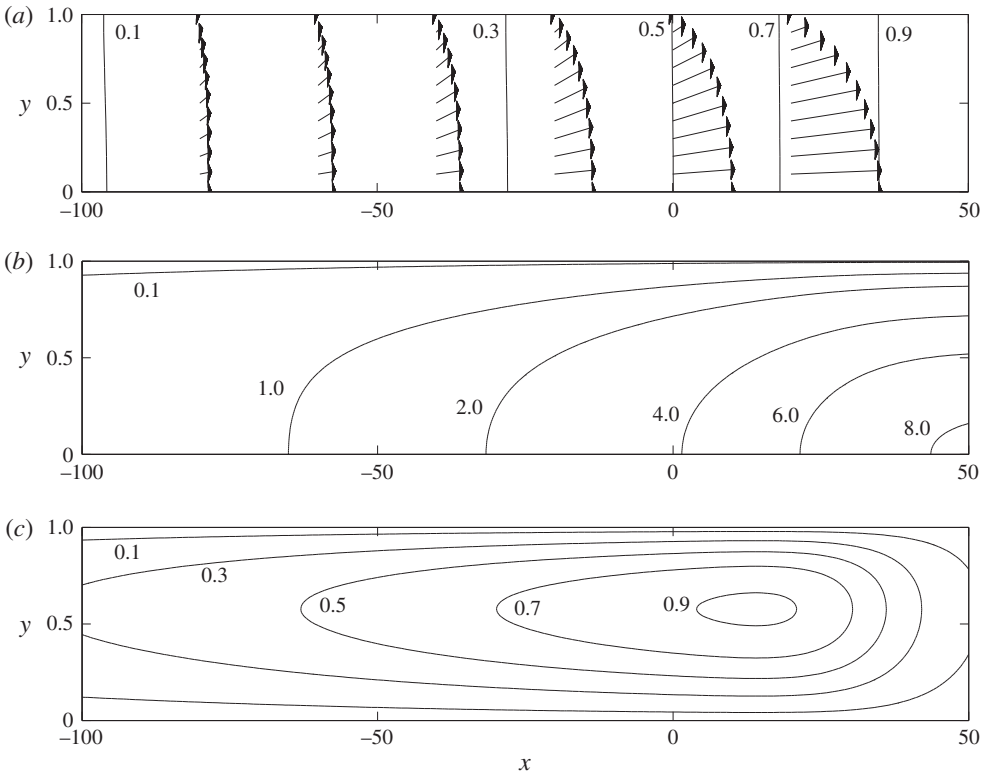

FIGURE 4. Contour plots of: (*a*) the temperature θ, with the velocity field induced by thermal expansion, which is given by $(u - \epsilon Pe(1 - y^2), v)$; (*b*) the horizontal velocity component due to thermal expansion, which is given by $u - \epsilon Pe(1 - y^2)$; (*c*) the vertical velocity component v. The values of the quantities along each contour are indicated. The plots correspond to $\epsilon = 50$, $Pe = 10$ and $\beta = 10$, and are plotted in the unscaled coordinates (x, y).

illustrates the gas expansion through the flame. Furthermore the figure demonstrates that the effective flame thickness increases with increasing Pe; this is in line with the asymptotic results (see the asymptotic formula (3.32) and also the discussion in the Conclusion section related to (6.3)).

Returning now to the effect of the Péclet number on the propagation speed, comparing the asymptotic result (4.18), derived in the constant-density approximation, with (4.14), derived in the variable-density case, provides a further reason for the larger effect of Pe on U_T in the constant-density case. The constant-density results are the same as the variable-density results, but with the term $Pe(1 - \alpha)$ replaced by Pe in the leading-order term for the effective propagation speed. (Note that the constant-density asymptotic results (4.15)–(4.17) are not recovered by simply setting $\alpha = 0$ in (3.29)–(3.31) due to the presence of α in the reaction term, which throughout this paper is set to $\alpha = 0.85$ in both cases.) This suggests that replacing the Péclet number in the variable-density case by a scaled Péclet number, given by

$$Pe_{scaled} = Pe(1 - \alpha), \tag{5.6}$$

would lead to strong agreement between the variable-density and constant-density numerical results.

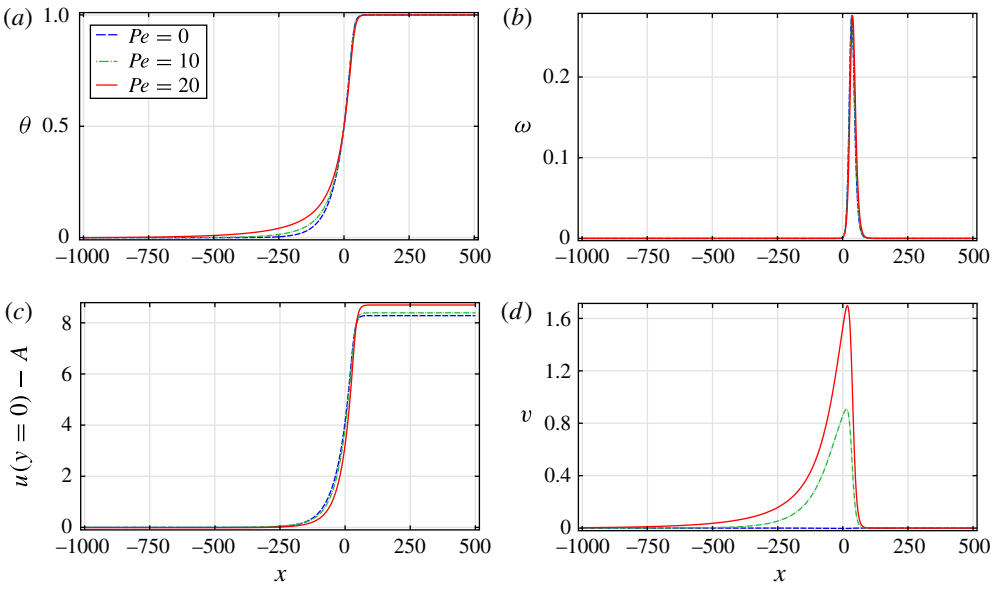

FIGURE 5. Plots of (*a*) temperature θ along $y = 0$; (*b*) reaction rate ω along $y = 0$; (*c*) increase in horizontal velocity u along $y = 0$ due to thermal expansion, which is given by $u(y = 0) - A$; (*d*) vertical velocity component v along $y = 0.5$. The plots correspond to selected values of the Péclet number Pe, with $\epsilon = 50$ and $\beta = 10$, and are plotted in the unscaled coordinates (x, y).

A plot of the numerically calculated value of U_T versus Pe_{scaled} in the constant-density and variable-density cases is given in figure 6. As expected, the relationship between U_T and Pe in the two cases is much more similar than in figure 2(*a*,*b*), but there is still a quantitative difference. This can be attributed to the fact that the finite activation energy has a more significant effect in the variable-density case than in the constant-density case, as described above. It is therefore expected that for larger values of β the agreement between the numerically calculated value of U_T and Pe_{scaled} would be closer between the two cases. To illustrate this, included in figure 6 is a comparison of U_T versus Pe_{scaled} from the numerical solution to (4.15)–(4.17) and (3.29)–(3.31), valid as $\epsilon \to \infty$, with $\beta = 30$. The figure shows that in this case the values of U_T in the constant- and variable-density cases are indeed closer together. However, performing numerical calculations of the full system with a larger value of β involves a significant amount of extra computation and is beyond the scope of this study.

Finally, it should be noted that the asymptotic results found in this paper agree with results obtained previously in the limit $Pe \to 0$. Expanding the constant-density result (4.18) as $Pe \to 0$ gives

$$U_T = 1 + \tfrac{4}{945} Pe^2 + O(Pe^3), \tag{5.7}$$

which agrees with Daou *et al.* (2002). Expanding the variable-density result (4.14) as $Pe \to 0$ gives

$$U_T = 1 + \tfrac{4}{945} Pe^2 (1 - \alpha)^2 + O(Pe^3). \tag{5.8}$$

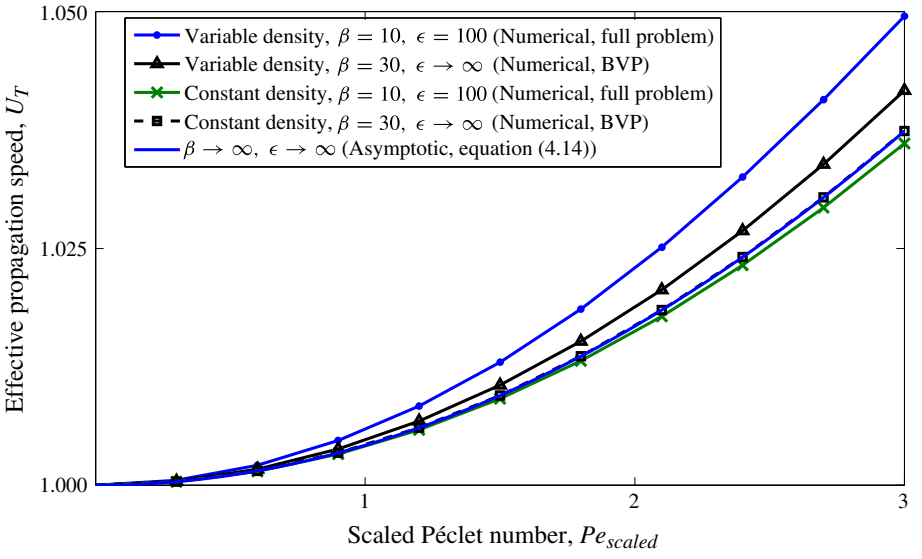

FIGURE 6. (Colour online) Comparison of numerical results for the effective propagation speed U_T versus the scaled Péclet number Pe_{scaled} in the variable-density and constant-density cases. Numerical simulations of the full system (2.7)–(2.15) are performed for the parameter values $Pr = 1$, $\alpha = 0.85$ and $\beta = 10$. Also included are numerical results of the solutions to (4.15)–(4.17) and (3.29)–(3.31) for $\alpha = 0.85$ and $\beta = 30$, to illustrate that for higher values of β the lines of U_T versus Pe_{scaled} in the constant-density and variable-density cases collapse onto the theoretical asymptotic curve.

This agrees with the results found by Short & Kessler (2009), which found $U_T \sim 1$ to leading order.

6. Conclusion

In this study we have investigated the propagation of a premixed flame through a narrow channel against a flow of large amplitude, taking the effect of the flame on the flow into account through the action of thermal expansion. This is the first study to consider a variable-density premixed flame in a narrow channel with Péclet number $Pe = O(1)$, which characterises the large-amplitude flow. It is also the first to investigate Taylor dispersion in the context of combustion. The problem has been studied analytically to determine the effective propagation speed U_T for $Pe = O(1)$, in the limit $\epsilon \to \infty$ with both finite and infinite values of the activation energy β. The asymptotic studies are complemented by a numerical study whose results have been compared to the analytical results to test their effectiveness.

It has been found that, in the limit $\epsilon \to \infty$, a two-dimensional premixed flame propagating through a rectangular channel against a Poiseuille flow can be described by a boundary value problem that corresponds to a one-dimensional premixed flame with an effective diffusion coefficient, given by

$$D_{eff} = D_T \left(1 + \frac{8}{945} Pe^2\right) \tag{6.1}$$

in the constant-density case, and

$$D_{eff} = D_T \left(1 + \frac{8}{945} Pe^2 \frac{\tilde{\rho}^2}{\tilde{\rho}_u^2}\right) \tag{6.2}$$

in the variable-density case. These values correspond to those found in studies of enhanced dispersion due to a Poiseuille flow in non-reactive fluids, known as Taylor dispersion. A premixed flame propagating through a channel in the limit $\epsilon \to \infty$, with $Pe = O(1)$ can therefore be considered to be in the Taylor regime.

Further, analytical solutions to the derived one-dimensional boundary value problems have been obtained in the limit $\beta \to \infty$ in both the constant-density and variable-density cases. The asymptotic results have been found to show strong agreement with the numerical results in both cases, as well as with results derived in previous studies in the limit $Pe \to 0$. Physical reasons for the differences between the constant- and variable-density cases in the relationship between the propagation speed and the Péclet number have been discussed.

The analytical results (4.14) and (4.18) can provide some insight towards understanding the effect of small-scale eddies on the propagation of a turbulent premixed flame, when the flow amplitude A in our study is identified with the turbulence intensity and the channel height L is identified with the turbulent flow (integral) scale. The situation where the flame is thick compared to the scale of the flow is described by Damköhler's second hypothesis, which may be stated in the form of a relationship between the dimensional effective propagation speed and the effective thermal diffusivity, given by $\tilde{U}_{eff} = \sqrt{D_{eff}/\tau}$. Here τ is the chemical time related to the planar premixed flame speed S_L^0 (used in this paper as unit speed to non-dimensionalise velocities) by $S_L^0 = \sqrt{D_T/\tau}$. Therefore on dividing these two equations, Damköhler's second hypothesis is recovered, to leading order, in (4.18), as can be seen by noting that

$$U_T \equiv \frac{\tilde{U}_{eff}}{S_L^0} = \sqrt{1 + \frac{8}{945} Pe^2} \equiv \sqrt{\frac{D_{eff}}{D_T}}. \tag{6.3}$$

The results (4.14) and (4.18) may also be used to provide a possible explanation of the so-called bending effect of the turbulent premixed flame speed when plotted in terms of the turbulence intensity for fixed values of the Reynolds number (see e.g. Bradley 1992; Ronney 1995). Therefore our distinguished limit, namely $\epsilon \to \infty$ with Pe fixed (note that the Reynolds number and Péclet number are equal if $Pr = 1$), mimics the experimental conditions of Bradley (1992) and can be used to shed some light on the experimental findings. However, we leave a full discussion of this specific turbulent combustion topic for future investigations given its unresolved and as yet controversial issues.

Finally, it has been shown that, in the limit $\epsilon \to \infty$, $\beta \to \infty$, the graphs of U_T in the constant- and variable-density cases are identical when plotted against a scaled Péclet number

$$Pe_{scaled} = Pe(1 - \alpha), \tag{6.4}$$

and graphs of the numerically calculated propagation speed against this scaled Péclet number have also been provided.

Appendix A. Cylindrical channel: asymptotic analysis in the limit $\epsilon \to \infty$

As in § 3, we consider the steady equations with $Le_F = 1$, so that only the temperature equation needs to be considered, since $y_F = 1 - \theta$. We consider the cylindrical coordinate system (r, z), with fluid velocity (u_r, u_z). In the limit $\epsilon \to \infty$, we introduce a rescaled coordinate

$$\xi = \frac{z}{\epsilon}, \tag{A 1}$$

so that the governing equations (2.7)–(2.11) become

$$\frac{\partial}{\partial \xi}\left(\rho(u_z + U)\right) + \epsilon \frac{1}{r}\frac{\partial}{\partial r}\left(\rho r u_r\right) = 0, \tag{A 2}$$

$$\rho(u_z + U)\frac{\partial u_z}{\partial \xi} + \epsilon \rho u_r \frac{\partial u_z}{\partial r} + \frac{\partial p}{\partial \xi} = Pr\left(\frac{4}{3}\frac{\partial^2 u_z}{\partial \xi^2} + \frac{\partial^2 u_z}{\partial r^2} + \frac{\epsilon^2}{r}\frac{\partial}{\partial r}\left(r\frac{\partial u_z}{\partial r}\right) + \frac{\epsilon}{3}\left(\frac{\partial^2 u_r}{\partial \xi \partial r} + \frac{1}{r}\frac{\partial u_r}{\partial \xi}\right)\right), \tag{A 3}$$

$$\rho(u_z + U)\frac{\partial u_r}{\partial \xi} + \epsilon \rho u_r \frac{\partial u_r}{\partial r} + \epsilon \frac{\partial p}{\partial r} = Pr\left(\frac{\partial^2 u_r}{\partial \xi^2} + \frac{4\epsilon^2}{3r}\frac{\partial}{\partial r}\left(r\frac{\partial u_r}{\partial r}\right) + \frac{\epsilon}{3r}\frac{\partial u_z}{\partial \xi}\right), \tag{A 4}$$

$$\rho(u_z + U)\frac{\partial \theta}{\partial \xi} + \epsilon \rho u_r \frac{\partial \theta}{\partial r} = \frac{\partial^2 \theta}{\partial \xi^2} + \frac{\epsilon^2}{r}\frac{\partial}{\partial r}\left(r\frac{\partial \theta}{\partial r}\right) + \frac{\omega}{1-\alpha}, \tag{A 5}$$

$$\rho = \left(1 + \frac{\alpha}{1-\alpha}\theta\right)^{-1}, \tag{A 6}$$

where

$$\omega = \frac{\beta^2}{2}\rho\,(1-\theta)\exp\left(\frac{\beta\,(\theta-1)}{1+\alpha\,(\theta-1)}\right). \tag{A 7}$$

These equations are subject to the boundary conditions

$$\frac{\partial \theta}{\partial r} = \frac{\partial y_F}{\partial r} = \frac{\partial u}{\partial r} = v = \frac{\partial p}{\partial r} = 0 \quad \text{at } r = 0, \tag{A 8}$$

$$\frac{\partial \theta}{\partial r} = \frac{\partial y_F}{\partial r} = u = v = 0 \quad \text{at } r = 1, \tag{A 9}$$

$$\theta = 0, \quad u_z = A(1 - r^2) = \epsilon Pe(1 - r^2), \quad u_r = 0 \quad \text{at } \xi = -\infty, \tag{A 10a–c}$$

$$\frac{\partial \theta}{\partial \xi} = \frac{\partial u}{\partial \xi} = \frac{\partial v}{\partial \xi} = p = 0 \quad \text{at } \xi = +\infty. \tag{A 11}$$

As in § 3, we now introduce expansions for $\epsilon \to \infty$ in the form

$$\left.\begin{aligned} &U = -\tfrac{1}{2}\epsilon Pe + U_0 + \epsilon^{-1}U_1 + \cdots, \\ &u_z = \epsilon u_0 + u_1 + \cdots, \quad u_r = v_0 + \epsilon^{-1}v_1 + \cdots, \\ &\theta = \theta_0 + \epsilon^{-1}\theta_1 + \cdots, \quad p = \epsilon^3 p_0 + \epsilon^2 p_1 + \cdots, \end{aligned}\right\} \tag{A 12}$$

where U_0 is the leading-order approximation to the effective flame speed U_T defined in (2.20), which in this case is given by

$$U_T \equiv U + \tfrac{1}{2}\epsilon Pe. \tag{A 13}$$

Substituting (A 12) into (A 2)–(A 5), to leading order we obtain

$$\frac{\partial}{\partial \xi}\left(\rho_0\left(u_0-\frac{1}{2}Pe\right)\right)+\frac{1}{r}\frac{\partial}{\partial r}\left(\rho_0 r v_0\right)=0, \tag{A 14}$$

$$\frac{\partial p_0}{\partial \xi}=\frac{Pr}{r}\frac{\partial}{\partial r}\left(r\frac{\partial u_0}{\partial r}\right), \tag{A 15}$$

$$\frac{\partial p_0}{\partial r}=0, \tag{A 16}$$

$$\frac{1}{r}\frac{\partial}{\partial r}\left(r\frac{\partial \theta_0}{\partial r}\right)=0. \tag{A 17}$$

Equations (A 16) and (A 17) can be integrated with respect to r to give $p_0=p_0(\xi)$ and $\theta_0=\theta_0(\xi)$, after considering the boundary conditions (A 8) and (A 9) on θ_0, so that $\rho_0=\rho_0(\xi)$ from (A 6).

Now we look for a separable solution for $u_0(\xi, y)$ in the form

$$u_0(\xi, r)=\hat{u}_0(r)\check{u}_0(\xi). \tag{A 18}$$

Substituting (A 18) into (A 15) gives

$$\frac{1}{r}\frac{\partial}{\partial r}\left(r\frac{\partial \hat{u}_0}{\partial r}\right)=\frac{1}{\check{u}_0 Pr}\frac{\partial p_0}{\partial \xi}, \tag{A 19}$$

where C is a constant. Equation (A 19) can be integrated twice with respect to r, using the boundary conditions (A 8) and (A 9), to yield

$$\hat{u}_0(r)=C(1-r^2), \tag{A 20}$$

so that

$$u_0(\xi, r)=\check{u}_0(\xi)(1-r^2), \tag{A 21}$$

where C has been absorbed into $\check{u}_0(\xi)$.

Integrating (3.11) with respect to r from $r=0$ to $r=1$, we obtain

$$\frac{\partial}{\partial \xi}\left(\rho_0(\xi)\left(\frac{1}{4}\check{u}(\xi)-\frac{1}{4}Pe\right)\right)=0, \tag{A 22}$$

after using boundary conditions (A 8) and (A 9) on v_0. Equation (A 22) implies that

$$\tfrac{1}{4}\rho_0(\xi)\left(\check{u}_0(\xi)-Pe\right)=\tfrac{1}{4}\left(\check{u}_0\left(\xi\rightarrow-\infty\right)-Pe\right)=0, \tag{A 23}$$

using the fact that $\rho_0(\xi\rightarrow-\infty)=1$ from (A 6) and boundary condition (A 10). Thus $\check{u}_0(\xi)=Pe$, so that

$$u_0=Pe(1-r^2). \tag{A 24}$$

Equation (A 14) can then integrated with respect to r, using (A 24) and condition (A 8), to yield

$$v_0=-\frac{1}{r\rho_0}\frac{\partial \rho_0}{\partial \xi}Pe\left(\frac{r^2}{4}-\frac{r^4}{4}\right). \tag{A 25}$$

Now, at $O(\epsilon)$ in (A 5) we have

$$\rho_0\left(u_0-\frac{1}{2}Pe\right)\frac{\partial\theta_0}{\partial\xi}=\frac{1}{r}\frac{\partial}{\partial r}\left(r\frac{\partial\theta_1}{\partial r}\right), \tag{A 26}$$

which, after using (A 24) and condition (A 8), can be integrated twice with respect to r to give

$$\theta_1=\rho_0\frac{\partial\theta_0}{\partial\xi}Pe\left(\frac{r^2}{8}-\frac{r^4}{16}\right)+\breve{\theta}_1(\xi). \tag{A 27}$$

Next we look to $O(1)$ in (A 2) to find

$$\frac{\partial}{\partial\xi}\left(\rho_1\left(u_0-\frac{1}{2}Pe\right)\right)+\frac{\partial}{\partial\xi}\left(\rho_0\left(u_1+U_0\right)\right)+\frac{1}{r}\frac{\partial}{\partial r}\left(\rho_0 v_1\right)+\frac{1}{r}\frac{\partial}{\partial r}\left(\rho_1 v_0\right)=0. \tag{A 28}$$

Equation (A 28) can be integrated first with respect to r from $r=0$ to $r=1$, utilising the boundary conditions (A 8) and (A 9) on v_0, and then with respect to ξ to give

$$\int_0^1 r\left(\rho_1\left(u_0-\frac{1}{2}Pe\right)\right)\mathrm{d}r+\int_0^1 r\left(\rho_0\left(u_1+U_0\right)\right)\mathrm{d}r=K. \tag{A 29}$$

To evaluate K, we use boundary conditions (A 10) to obtain

$$\begin{aligned}K\;=\;&\int_0^1 r\left(\rho_1(\xi\to-\infty)\left(u_0(\xi\to-\infty)-\frac{1}{2}Pe\right)\right)\mathrm{d}r\\&+\int_0^1 r\left(\rho_0(\xi\to-\infty)\left(u_1(\xi\to-\infty)+U_0\right)\right)\mathrm{d}r=\frac{U_0}{2}.\end{aligned} \tag{A 30}$$

Finally, at $O(1)$ of (A 5) we have

$$\begin{aligned}&\rho_0\left(u_1+U_0\right)\frac{\partial\theta_0}{\partial\xi}+\rho_1\left(u_0-\frac{1}{2}Pe\right)\frac{\partial\theta_0}{\partial\xi}+\rho_0\left(u_0-\frac{1}{2}Pe\right)\frac{\partial\theta_1}{\partial\xi}+\rho_0 v_0\frac{\partial\theta_1}{\partial r}\\&=\frac{\partial^2\theta_0}{\partial\xi^2}+\frac{1}{r}\frac{\partial}{\partial r}\left(r\frac{\partial\theta_2}{\partial r}\right)+\frac{\omega_0}{1-\alpha},\end{aligned} \tag{A 31}$$

where $\omega_0(\xi)=\omega(\theta_0,\,\rho_0)$. Integrating (A 31) with respect to r from $r=0$ to $r=1$, noting the boundary conditions (A 8) and (A 9) on θ and substituting (A 24), (A 25), (A 27), (A 29) and (A 30) leads to

$$U_0\frac{\partial\theta_0}{\partial\xi}-\frac{\partial}{\partial\xi}\left(\left(1+\frac{1}{192}Pe^2\rho_0^2\right)\frac{\partial\theta_0}{\partial\xi}\right)=\frac{\omega_0}{1-\alpha}, \tag{A 32}$$

with

$$\left.\begin{aligned}\rho_0&=\left(1+\frac{\alpha}{1-\alpha}\theta_0\right)^{-1},\\\omega_0&=\frac{\beta^2}{2}\rho_0\left(1-\theta_0\right)\exp\left(\frac{\beta\left(\theta_0-1\right)}{1+\alpha\left(\theta_0-1\right)}\right),\end{aligned}\right\} \tag{A 33}$$

subject to the boundary conditions

$$\theta_0(-\infty)=0,\quad \theta_{0\xi}(+\infty)=0. \tag{A 34a,b}$$

REFERENCES

AHN, J., EASTWOOD, C., SITZKI, L. & RONNEY, P. D. 2005 Gas-phase and catalytic combustion in heat-recirculating burners. *Proc. Combust. Inst.* **30** (2), 2463–2472.

ALDREDGE, R. C. 1992 The propagation of wrinkled premixed flames in spatially periodic shear flow. *Combust. Flame* **90** (2), 121–133.

BRADLEY, D. 1992 How fast can we burn? In *Symposium (International) on Combustion*, vol. 24, pp. 247–262. Elsevier.

BRENNER, H. & EDWARDS, D. A. 1993 *Macrotransport Processes*. Butterworth-Heinemann.

CLAVIN, P. & WILLIAMS, F. A. 1979 Theory of premixed-flame propagation in large-scale turbulence. *J. Fluid Mech.* **90** (3), 589–604.

CUI, C., MATALON, M., DAOU, J. & DOLD, J. 2004 Effects of differential diffusion on thin and thick flames propagating in channels. *Combust. Theor. Model.* **8** (1), 41–64.

DAMKÖHLER, G. 1940 Influence of turbulence on the velocity flames in gas mixtures. *Z. Elektrochem.* **46**, 601–626.

DAOU, J., DOLD, J. & MATALON, M. 2002 The thick flame asymptotic limit and Damköhler's hypothesis. *Combust. Theor. Model.* **6** (1), 141–153.

DAOU, J. & MATALON, M. 2001 Flame propagation in Poiseuille flow under adiabatic conditions. *Combust. Flame* **124** (3), 337–349.

DAOU, J. & MATALON, M. 2002 Influence of conductive heat-losses on the propagation of premixed flames in channels. *Combust. Flame* **128** (4), 321–339.

DAOU, J. & SPARKS, P. 2007 Flame propagation in a small-scale parallel flow. *Combust. Theor. Model.* **11** (5), 697–714.

DENTZ, M., TARTAKOVSKY, D. M., ABARCA, E., GUADAGNINI, A., SANCHEZ-VILA, X. & CARRERA, J. 2006 Variable-density flow in porous media. *J. Fluid Mech.* **561**, 209–235.

DEUFLHARD, P. 1974 A modified Newton method for the solution of ill-conditioned systems of nonlinear equations with application to multiple shooting. *Numer. Math.* **22** (4), 289–315.

FAN, A., MINAEV, S., KUMAR, S., LIU, W. & MARUTA, K. 2007 Experimental study on flame pattern formation and combustion completeness in a radial microchannel. *J. Micromech. Microengng* **17** (12), 2398.

FELDER, C., OLTEAN, C., PANFILOV, M. & BUÈS, M. 2004 Dispersion de Taylor généralisée à un fluide à propriétés physiques variables. *C. R. Méc.* **332** (3), 223–229.

FERNANDEZ-PELLO, A. C. 2002 Micropower generation using combustion: issues and approaches. *Proc. Combust. Inst.* **29** (1), 883–899.

KANURY, A. M. 1975 *Introduction to Combustion Phenomena: For Fire, Incineration, Pollution, and Energy Applications,* vol. 2. Taylor & Francis.

KERSTEIN, A. R., ASHURST, W. T. & WILLIAMS, F. A. 1988 Field equation for interface propagation in an unsteady homogeneous flow field. *Phys. Rev.* A **37** (7), 2728–2731.

KURDYUMOV, V. N. 2011 Lewis number effect on the propagation of premixed flames in narrow adiabatic channels: symmetric and non-symmetric flames and their linear stability analysis. *Combust. Flame* **158** (7), 1307–1317.

KURDYUMOV, V. N. & FERNANDEZ-TARRAZO, E. 2002 Lewis number effect on the propagation of premixed laminar flames in narrow open ducts. *Combust. Flame* **128** (4), 382–394.

KURDYUMOV, V. N. & MATALON, M. 2013 Flame acceleration in long narrow open channels. *Proc. Combust. Inst.* **34** (1), 865–872.

LECONTE, M., JARRIGE, N., MARTIN, J., RAKOTOMALALA, N., SALIN, D. & TALON, L. 2008 Taylor's regime of an autocatalytic reaction front in a pulsative periodic flow. *Phys. Fluids* **20**, 057102.

OLTEAN, C., FELDER, CH., PANFILOV, M. & BUÈS, M. A. 2004 Transport with a very low density contrast in Hele–Shaw cell and porous medium: evolution of the mixing zone. *Transp. Porous Media* **55** (3), 339–360.

PEARCE, P. & DAOU, J. 2013*a* The effect of gravity and thermal expansion on the propagation of a triple flame in a horizontal channel. *Combust. Flame* **160** (12), 2800–2809.

PEARCE, P. & DAOU, J. 2013*b* Rayleigh–Bénard instability generated by a diffusion flame. *J. Fluid Mech.* **736**, 464–494.

PETERS, N. 2000 *Turbulent Combustion*. Cambridge University Press.

RONNEY, P. D. 1995 Some open issues in premixed turbulent combustion. In *Modeling in Combustion Science* (ed. J. Buckmaster & T. Takeno), pp. 1–22. Springer.

SHAMPINE, L. F., KIERZENKA, J. & REICHELT, M. W. 2000 Solving boundary value problems for ordinary differential equations in MATLAB with BVP4C. *Tech. Rep.* The MathWorks.

SHORT, M. & KESSLER, D. A. 2009 Asymptotic and numerical study of variable-density premixed flame propagation in a narrow channel. *J. Fluid Mech.* **638**, 305–337.

SITZKI, L., BORER, K., SCHUSTER, E., RONNEY, P. D. & WUSSOW, S. 2001 Combustion in microscale heat-recirculating burners. In *The Third Asia-Pacific Conference on Combustion, Seoul, Korea*, vol. 6, pp. 11–14.

SIVASHINSKY, G. I. 1988 Cascade-renormalization theory of turbulent flame speed. *Combust. Sci. Technol.* **62** (1–3), 77–96.

ATAYLOR, G. 1953 Dispersion of soluble matter in solvent flowing slowly through a tube. *Proc. R. Soc. Lond.* **219** (1137), 186–203.

YAKHOT, V. 1988 Propagation velocity of premixed turbulent flames. *Combust. Sci. Technol.* **60** (1–3), 191–214.